A Comprehensive Analysis of Hydrogen Bond Interactions Based on Local Vibrational Modes

Marek Freindorf, Elfi Kraka,* and Dieter Cremer

Local stretching modes for 69 different DH single bonds and 58 H···A H-bonds are calculated at the ωB97X-D/aug-cc-pVTZ level of theory to describe the changes in donor D and acceptor A upon forming the hydrogen-bonded complex. The intrinsic strength of the DH and AH interactions is determined utilizing the properties of a well-defined set of local, uncoupled vibrational modes. The local mode stretching force constant $k_a(HA)$ provides a unique measure of bond strength for both covalently and electrostatically bonded complexes. Generally applicable bond orders are derived, which can be related to the binding energies of the hydrogen bonded complexes. Although the red shifts in the DH stretching frequencies can be used to detect hydrogen bonding, they are not sufficient to assess the strength of hydrogen bonding. It is demonstrated that the calculated BSSE-corrected binding energies of hydrogen bonded complexes are related to the sum of bond order changes caused by hydrogen bonding. The covalent character of charge assisted hydrogen bonds is explained. Because local mode frequencies can also be derived from experimental normal mode frequencies, a new dimension in the study of hydrogen bonding is gained. © 2012 Wiley Periodicals, Inc.

DOI: 10.1002/qua.24118

Introduction

The properties of the $3N - L$ normal vibrational modes of an N-atomic molecule (L: number of translational and rotational motions of the molecule) contain important electronic structure information. However, it is difficult to decode this information into individual atom–atom interactions (e.g., those resulting in bonding) because normal vibrational modes are always delocalized due to the coupling of the motions of the atoms within the molecule. Experimentalists have repeatedly attempted to determine local vibrational modes for polyatomic molecules, however, only with limited success.[1–7] More successful were theoretical attempts to determine local vibrational modes. Konkoli and Cremer[8,9] developed in 1998 a unique way of extracting local vibrational modes, which do no longer couple, from delocalized normal modes. These modes were dubbed by the authors adiabatic (relaxed) internal coordinate modes (AICoMs).[8] They showed that local vibrational modes are perfectly suited to describe chemical bonding, which was exploited in a number of investigations.[9–15]

Recently, it was shown[16] that the AICoMs of Cremer and Konkoli are the unique and only local counterparts of the $3N - L$ normal vibrational modes, which according to their properties (frequency and force constant) correspond exactly to those local modes, which could be determined experimentally in a few cases.[1–7] The AICoMs can be calculated for hamonic vibrational modes, anharmonically corrected vibrational modes, or measured vibrational modes.[11] They have been used to describe various situations of covalent or ionic bonding[10,11,13,14] as well as the breaking (forming) of chemical bonds in chemical reactions.[15,17,18] In this work, we will extend their use to weakly covalent and/or noncovalent bonding situations as they occur in H-bonded complexes.

Since the discovery of hydrogen bonding (HB) more than 100 years ago, the myriad of experimental and computational investigations focusing on HB has been repeatedly discussed in books[19–24] and numerous review articles only some of which can be mentioned here.[25–31] Recently, Gilli and Gilli[24] summarized the experimental means of investigating HB. Despite all experimental work on HB, it is fair to say that computational methods have led to an improved understanding of the electronic nature of the HB. Early investigations focused preferentially on the electrostatic character of the HB[24] whereas in the more recent investigations both electrostatic, covalent, and even dispersion contributions to HB have been analyzed. There is no longer any doubt that a detailed description of HB can only be obtained by using reliable quantum chemical methods.[21,23–25,31]

Important tools for a quantum chemical investigation of the HB have been the energy decomposition analysis,[32–34] the virial and topological analysis of the total electron density distribution,[35–37] the analysis of the energy density distribution,[38–42] the natural orbital population analysis,[43,44] or the electron localization analysis of Becke and Edgecombe.[45,46] Especially the electron density analysis of HB has led to new, sometimes even contradictory insights into HB. In this connection, the work by Koch and Popelier,[47] Knop et al.,[48] Grabowski,[49] Espinoza and coworkers,[50] Gatti and Macchi[51] has to be mentioned. A description of HB utilizing electron localization functions (ELF) was advocated by Fuster and Silvi.[52,53] Recently, the analysis of the electrostatic potential[54] or even that of the reduced electron density gradient was used to describe HB.[55]

M. Freindorf, E. Kraka, D. Cremer
Department of Chemistry, Southern Methodist University, 3215 Daniel Ave, Dallas, Texas 75275-0314
E-mail: ekraka@gmail.com

Contract grant sponsor: National Science Foundation; contract grant number: CHE 071893.

Alternatively to the investigation of the equilibrium geometry of the HB complex, the energy profile of the proton transfer process from donor D to acceptor A was studied and a characterization of different HB situations accomplished.[30,56] Based on this approach, the proton affinity (PA) and pK_a equilibration concepts of HB were established, which connect the binding energy ΔE of a HB-complex to the differences $PA(DH) - PA(HA)$ or $pK_a(DH) - pK_a(HA)$.[30,56] Proton transfer probes the strength of HB, however leads also to a drastic change in the electronic structure of the HB complex, which makes its analysis problematic (see later). Changes in the electronic nature of HB are less drastic when applying an external electric field and accordingly provide valuable information on HB.[57,58] Related to this approach is the study of magnetic electron currents in HB complexes as a response to a magnetic field.[59]

In this work, we will carry out a dynamic investigation of HB based on the vibrational modes of a HB complex. Vibrational properties such as stretching frequencies and stretching force constants relate to infinitesimally small changes in HB and therefore provide measures of its strength without changing the electronic structure of the HB complex. In this way, questions concerning the character of HB in special complexes (covalent or electrostatic), the exact influence of donor D and acceptor A, or stereoelectronic factors influencing the strength of the HB can be investigated.

Use of Vibrational Spectroscopy for the Description of H-Bonding

Vibrational spectroscopy has been amply used to describe HB.[26,60–72] The DH bond is weakened as a result of HB, which is revealed by a red shift $\Delta\omega(DH) = \omega(DH, \text{complex}) - \omega(DH, \text{monomer})$ of the DH stretching frequency $\omega(\text{monomer})$ of the monomer *RDH* when forming a HB complex $RDH \cdots AR'$ (in the following the HB complex is abbreviated as *DHA* indicating for the two monomers just the *DH* and *A* part). Experimentally as well as computationally the value of $\Delta\omega(DH)$ and its frequency-normalized analogue $\eta(DH) = \Delta\omega(DH)/\omega(DH, \text{monomer})$ have been determined and used as a signature for HB.[70,72,73] It is tempting to relate $\Delta\omega(DH)$ to the thermochemical strength of the HB. However, the DH stretching mode in a HB complex DHA will couple to other vibrational modes of the complex and thereby delocalize. Therefore, one cannot expect that experimentally determined $\Delta\omega(DH)$ or $\eta(DH)$ values are reliable descriptors of HB. Apart from this, there are also problems in connection with the choice of the DH reference frequency needed for determining $\Delta\omega(DH)$.

For example, if water is involved in HB as a donor molecule, the symmetric and antisymmetric OH stretching modes will decouple to some extent. The value $\Delta\omega$ for OH stretching can be based either on the symmetric or the antisymmetric OH stretching or their average. For convenience, $\Delta\omega(DH)$ values are based on a comparison of complex and monomer frequencies, which are closest in value. This however does not imply that the smallest $\Delta\omega(DH)$ difference is the proper measure for the strength of HB. Apart from this, residual couplings between DH and AH stretching modes can alter the magnitude of the measured red shift in the DH stretching frequency.[65] These problems can become even more serious in the case of complexes forming a cyclic system due to multiple HBs. In summary, vibrational spectroscopy, although an important tool for identifying and characterizing HB, does not provide a reliable tool for determining the strength of the HB as long as delocalized normal vibrational modes are used.

A direct descriptor of HB could be the HA stretching frequency, which of course has often a low value and intensity and therefore is more difficult to measure than the DH stretching mode. Local vibrational modes solve the problems, which accompany the description of HB with the help of vibrational spectroscopy. The local HA stretching mode and its associated stretching force constant can be directly determined and related to the strength of the HB.[11] Quantum chemical investigations based on anharmonically corrected vibrational frequencies[74] suggest that local stretching force constants obtained with the harmonic approximation provide a reliable descriptor of the relative HB strength.

Of course, the local stretching force constants cannot lead to a distinction between covalent and electrostatic HBs. For this purpose, one needs a second information where in this work the local energy density distribution is used. Cremer and Kraka[38–40] showed that covalent bonding implies a stabilizing (negative) energy density $H(\mathbf{r})$ at the bond critical point $\mathbf{r}_c(AB)$ of the electron density distribution $\rho(\mathbf{r})$ between two bonded atoms A and B. The energy density distribution $H_c = H(\mathbf{r}_c)$ will be close to zero or positive if the interactions are noncovalent, i.e., of the electrostatic or dispersion type. Espinoza and coworkers[41,42] have confirmed the usefulness of this approach in the case of HB.

In this work, we will investigate the HB complexes shown in Figure 1 as well as 11 monomers that function as suitable reference molecules utilizing the local vibrational modes and the properties of the energy density distribution. Results of this investigation will be presented in the following way. In "Computational Methods" section, we will sketch the theory of the local vibrational modes and describe the computational methods used in this work. Results and their discussion will be presented in "Results and Discussion" section. Finally, in "Conclusion" section the conclusions of this investigation are drawn.

Computational Methods

By solving the Euler-Lagrange equations for a vibrating molecule, the basic equation of vibrational spectroscopy given by Eq. (1) is obtained:[75]

$$\mathbf{F^q D} = \mathbf{G}^{-1}\mathbf{D}\boldsymbol{\Lambda} \tag{1}$$

where **F** is the force constant matrix and **D** contains the normal mode vectors $\mathbf{d}_\mu$ ($\mu = 1, \ldots, N_{vib}$ with $N_{vib} = 3K - L$) given as column vectors. Both matrices are expressed in terms of internal coordinates **q**. Matrix **G** is the Wilson matrix and matrix $\boldsymbol{\Lambda}$ is a diagonal matrix containing the vibrational eigenvalues $\lambda_\mu = 4\pi^2 c^2 \omega_\mu^2$ where ω_μ represents the (harmonic) vibrational

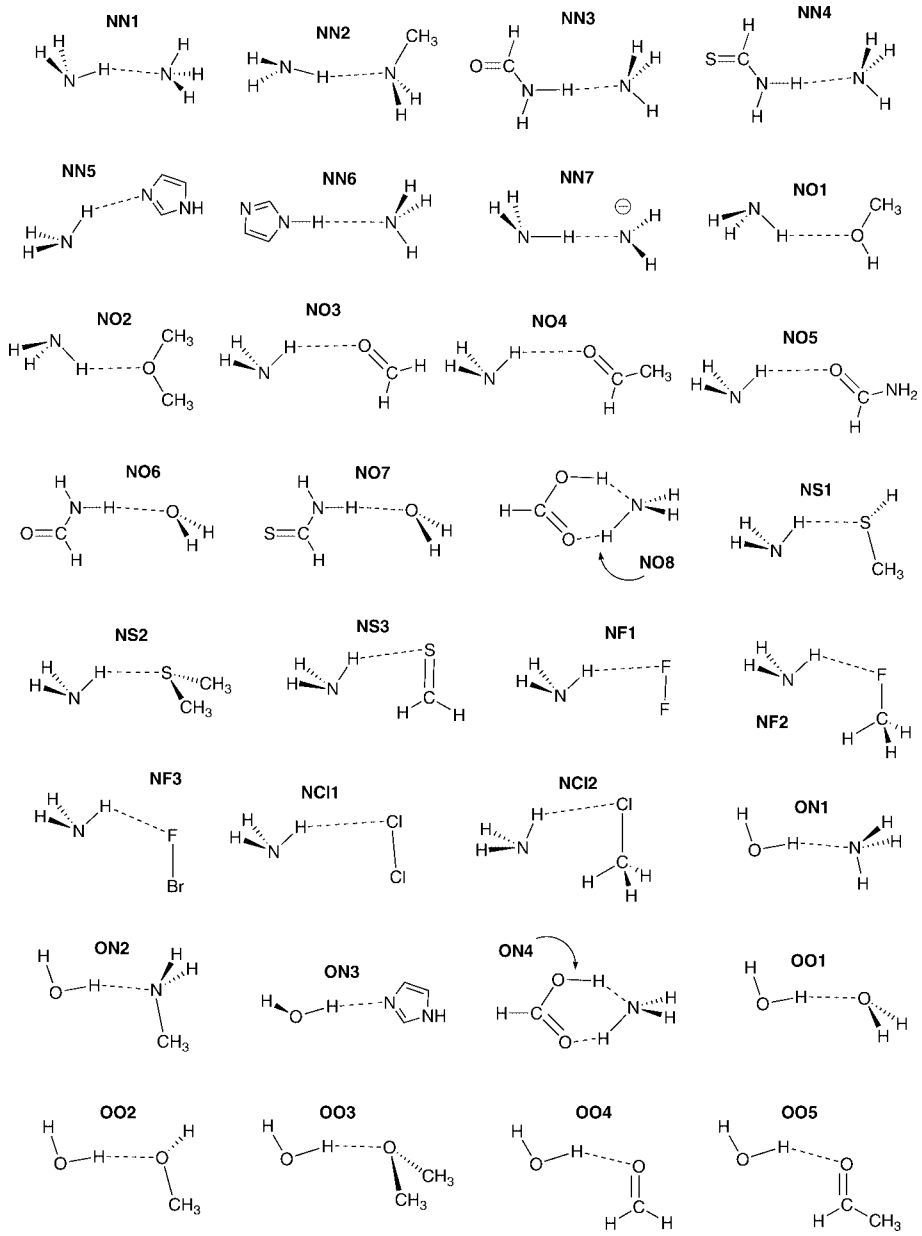

Figure 1. Structures and symbols of the HB systems and the corresponding monomers investigated in this work. HB is indicated by a dashed line. Conformations are given schematically as calculated.

frequency of mode $\mathbf{d}_\mu$ given in reciprocal *cm* and *c* is the speed of light. The vibrational problem requires the calculation of the analytical second derivatives of the molecular energy and therefore it is solved in terms of Cartesian coordinates

$$\mathbf{f^x L} = \mathbf{ML\Lambda} \tag{2}$$

where $\mathbf{f^x}$ is the force constant matrix, **L** collects the vibrational eigenvectors $\mathbf{l}_\mu$, and **M** is the mass matrix of the molecule in question. The force constant matrix can be written in three different ways using either Cartesian coordinates, internal coordinates **q** or normal coordinates **Q**:

$$\mathbf{F^q} = \mathbf{C}^\dagger\mathbf{f^x C} \tag{3}$$

$$\mathbf{F^Q} = \mathbf{K} = \mathbf{L}^\dagger\mathbf{f^x L} \tag{4}$$

Matrix **C** transforms normal mode eigenvectors from internal coordinate space to Cartesian space

$$\mathbf{l}_\mu = \mathbf{C}\mathbf{d}_\mu \tag{5}$$

and is given by

$$\mathbf{C} = \mathbf{M}^{-1}\mathbf{B}^\dagger\mathbf{G}^{-1} \tag{6}$$

The elements of the **B** matrix are defined by the partial derivatives of internal coordinates with regard to Cartesian coordinates.[75] Matrices **B** and **C** are closely related:

$$\mathbf{BC} = \mathbf{BM}^{-1}\mathbf{B}^\dagger\mathbf{G}^{-1} = \mathbf{GG}^{-1} = \mathbf{I} \tag{7}$$

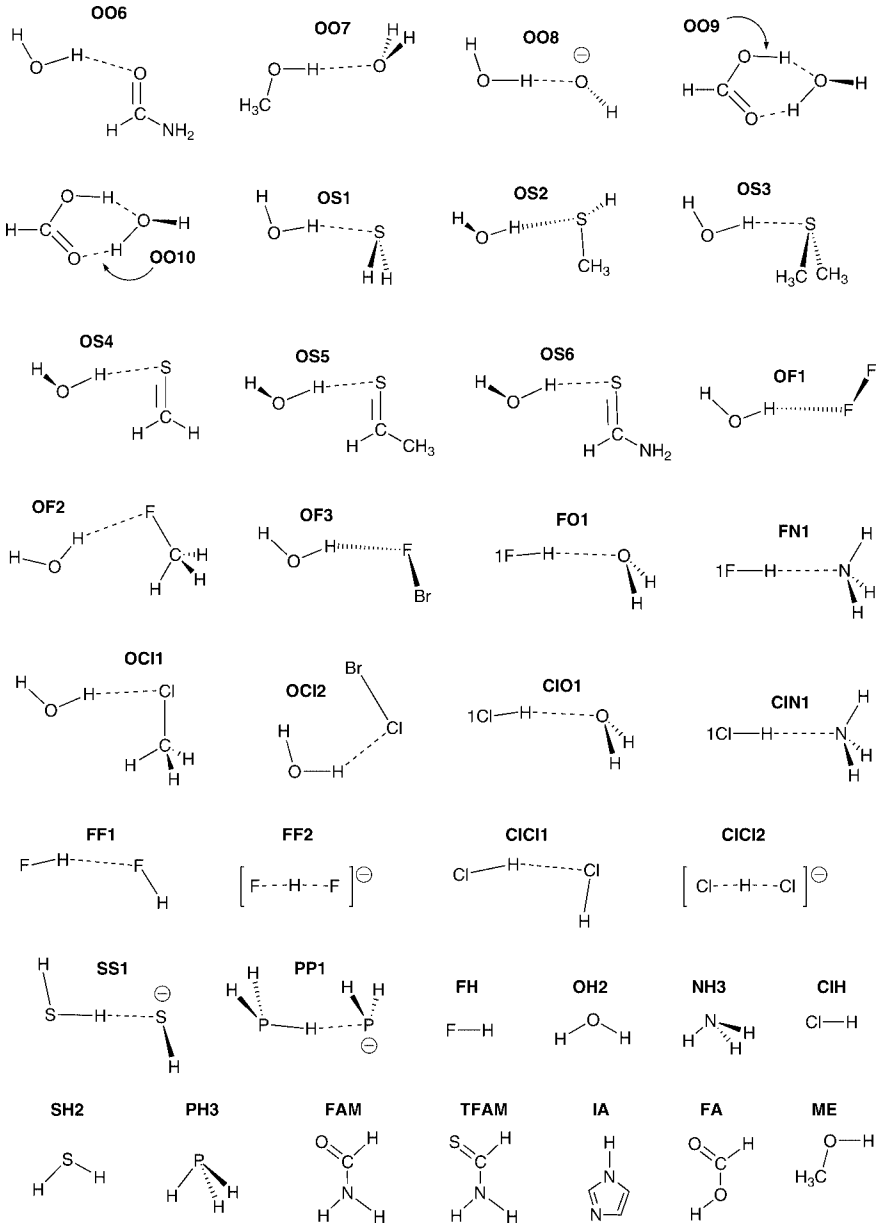

Figure 1. (Continued)

because $\mathbf{G} = \mathbf{B}\mathbf{M}^{-1}\mathbf{B}^{\dagger}$. Konkoli and Cremer[8] determined the local vibrational modes directly from the Euler-Lagrange equations by setting all masses equal to zero with the exception of those of the molecular fragment (e.g., bond AB) carrying out a localized vibration. They proofed that this is equivalent to requiring an adiabatic relaxation of the molecule after enforcing a local displacement of the atoms by changing a specific internal coordinate as, e.g., a bond length in the case of a diatomic molecular fragment (leading parameter principle).[8] The local modes obtained in this way take the form:[8]

$$\mathbf{a}_i = \frac{\mathbf{K}^{-1}\mathbf{d}_i}{\mathbf{d}_i\mathbf{K}^{-1}\mathbf{d}_i^{\dagger}} \tag{8}$$

where subscript i specifies an internal coordinate q_i and the local mode is expressed in terms of normal coordinates $\mathbf{Q}$ associated with force constant matrix $\mathbf{K}$ of Eq. (4). The local mode force constant k_a is obtained from Eq. (9):

$$k_a = \mathbf{a}_i^{\dagger}\mathbf{K}\mathbf{a}_i = \left(\mathbf{d}_i\mathbf{K}^{-1}\mathbf{d}_i^{\dagger}\right)^{-1} \tag{9}$$

Local mode force constants, contrary to normal mode force constants, have the advantage of being independent of the choice of the coordinates used to describe the molecule in question. Already at an early stage of vibrational spectroscopy it was shown that a change in the coordinates leads also to a change in the normal mode force constants.[75,76] Although the vibrational frequencies are not influenced by the choice of the coordinates, they cannot provide reliable bond or electronic structure information because of the delocalized nature of the normal vibrational modes and their dependence on the masses of the atoms involved in a vibration.

In 1963, Decius[76] was the first who tried to obtain local mode information from normal vibrational modes. He realized that the inverse of the force constant matrix $(\mathbf{F}^q)^{-1} = \mathbf{\Gamma}^q$ possesses diagonal elements Γ_{ii}, which turned out to be independent of the choice of the coordinates[77] and seemed to be typical of the electronic nature of a molecular fragment described by the internal coordinate q_i. Since the early work of Decius, parameters Γ_{ii}, later called compliance constants,[78] have found some use when describing chemical bonds.[79,80]

Compliance constants are not observable quantities. They are not associated with a vibrational mode or a measurable quantity of vibrational spectroscopy. Also, they provide an unusual measure of the bond strength by quantifying its weakness, i.e., the larger the value of Γ_{ii} the weaker is the associated bond. Finally, their interpretation is hampered by the fact that two compliance constants Γ_{ii} and Γ_{jj} are connected by an off-diagonal element Γ_{ij} of finite magnitude, the meaning of which and its consideration in connection with the diagonal compliance constants remains unclear.[81]

Recently, Zou et al.[16] have proven that compliance constants are nothing else but the reciprocal of the local mode force constants of Konkoli and Cremer.[8] Utilizing Eqs. (3)–(5), the internal coordinate force constant matrix can be written as

$$\mathbf{F}^q = (\mathbf{D}^{-1})^\dagger \mathbf{L}^\dagger \mathbf{f}^x \mathbf{L} \mathbf{D}^{-1} = (\mathbf{D}^{-1})^\dagger \mathbf{K} \mathbf{D}^{-1} \tag{10}$$

Hence, the inverse force constant matrix, i.e., the compliance matrix $\mathbf{\Gamma}^q$, and its diagonal elements are given by

$$\mathbf{\Gamma}^q = (\mathbf{F}^q)^{-1} = \mathbf{D}\mathbf{K}^{-1}\mathbf{D}^\dagger \tag{11}$$

$$(\mathbf{\Gamma}^q)_{ii} = \mathbf{d}_i \mathbf{K}^{-1} \mathbf{d}_i^\dagger \tag{12}$$

which proves that

$$k_a = 1/(\mathbf{\Gamma}^q)_{ii}, \tag{13}$$

i.e., the inverse of the local mode force constants of Konkoli and Cremer are the compliance constants of Decius.[76] This proof has two important implications. (i) The AICoM local modes are the only local modes that are directly related to the normal vibrational modes of a molecule. (ii) The compliance constants are superfluous as bond descriptors because the local mode force constants already fulfill this task and there is no reason for working with the reciprocal of a force constant for the purpose of describing the weakness of a chemical bond.

In this work, we calculate the local mode stretching force constants associated with the HB to quantify DH bond weakening and HA bond formation. Despite the many flaws of density functional theory (DFT) in the case of weak noncovalent interactions[25,82,83] it has been shown that a reasonable account of HB will be obtained if the XC functional is carefully chosen, a large augmented basis set is used, and all energy calculations and geometry optimizations are carried out using basis set superposition error (BSSE) corrections.[84] Accordingly, we employed the long-range corrected hybrid density functional ωB97X-D, which includes empirical dispersion corrections,[85,86] in connection with the aug-cc-pVTZ basis set of Dunning.[87,88] In addition, we used for all geometry and energy calcullations the counterpoise correction of the BSSE.[89,90] Sherill and coworkers showed that for counterpoise-corrected ωB97X-D calculations HB binding energies ΔE close to reliable CCSD(T) results are obtained.[84]

Energy, geometry, and vibrational frequency calculations were performed with an ultrafine grid for numerical integrations. All calculated stationary points were verified as minima by the eigenvalues of the Hessian matrix of the molecular energy. Calculations were carried out with the quantum chemical program packages COLOGNE11,[91] Gaussian09,[92] and AIMAII.[93]

Results and Discussion

In Table 1, properties of the DH and HA bond of 58 HB complexes and 11 monomers calculated at the ωB97X-D/aug-cc-pVTZ level of theory are listed. These comprise the distance values $R(DH)$ and $R(HA)$, the corresponding local mode force constants and local mode frequencies, the shift values $\Delta\omega_a(DH)$ and $\Delta k_a(DH)$, the corresponding frequency (or force constant)-normalized shift values, the binding energies ΔE, the density properties ρ_c, H_c, and H_c/ρ_c as well as the calculated bond orders $n(DH)$ and $n(HA)$. Correlations between some of these properties are shown in Figures 2–4.

Conventional descriptors of H-bond strength

Among chemists, there is a tendency of relating the bond length R to the bond strength and accordingly there have been attempts of getting an insight into HB directly from distance values $R(HA)$ or indirectly from changes in $R(DH)$ values upon HB formation.[26,48,49,94] Badger[95] was the first who showed that the stretching force constants of diatomic molecules are suitable bond strength descriptors and are related to the bond length via a power relationship. Relationships $k = f(R)$ for different bond types can be merged into a single one by using an effective bond length $R_{eff}(XY) = R(XY) - d(X) - d(Y)$ where the correction parameter d represents an electron density compressibility limit depending on the number of core shells of a bonded atom.[14] In the literature, these force constant-bond length relationships are known as Badger's rule.[95] Recently, Kraka, Larsson, and Cremer (KLC) succeeded in generalizing the Badger's rule from diatomic to polyatomic molecules utilizing the AICoM local mode force constants.[14]

In Figure 2a, k_a values are shown in dependence of R where the large k_a values (>3 mdyn/Å) are typical of covalent DH bonds and the small k_a values (<1 mdyn/Å) represent HB between DH and the acceptor A. Two exponential curves are shown in Figure 2a: the first represents DH or AH interactions with D and A being second period atoms and the second those involving third period atoms such as P, S, or Cl. Inspection of special DH bonds such as NH or OH (Fig. 2b) confirms that the Badger's rule for polyatomic molecules is fulfilled as previously pointed out by KLC.[14] However, in the region of HB (Fig. 2c), there is a relatively strong scattering of data points, which does not become obvious from Figure 2a because changes in the HB

Table 1. Properties of hydrogen bonded complexes as calculated at the ωB97X-D/aug-cc-pVTZ level of theory.[a]

Molecule	Bond	R	k_a	Δk_a	$\Delta k_a/k_a$	ω_a	$\Delta\omega_a$	$\Delta\omega_a/\omega_a$	ΔE	ρ_c	H_c	H_c/ρ_c	n
NN1	N–H	1.017	6.692	−0.300	−0.043	3476	−77	−0.022		2.302	−3.434	−1.492	0.902
	H···N	2.250	0.110			446			−3.18	0.110	0.008	0.072	0.288
NN2	N–H	1.018	6.617	−0.375	−0.054	3456	−97	−0.027		2.297	−3.421	−1.489	0.900
	H···N	2.217	0.105			435			−3.90	0.119	0.007	0.061	0.284
NN3	N–H	1.016	6.561	−1.057	−0.139	3442	−266	−0.072		2.287	−3.750	−1.640	0.897
	H···N	2.052	0.158			534			−6.90	0.171	−0.006	−0.036	0.318
NN4	N–H	1.020	6.313	−1.216	−0.162	3376	−311	−0.084		2.271	−3.746	−1.650	0.888
	H···N	2.003	0.193			590			−8.05	0.191	−0.013	−0.068	0.337
NN5	N–H	1.017	6.706	−0.286	−0.041	3479	−74	−0.021		2.303	−3.429	−1.489	0.903
	H···N	2.239	0.078			374			−4.85	0.105	0.011	0.108	0.262
NN6	N–H	1.020	6.335	−1.258	−0.166	3382	−320	−0.086		2.272	−3.819	−1.681	0.889
	H···N	1.991	0.211			617			−8.02	0.195	−0.016	−0.079	0.345
NN7	N–H	1.058	3.810	−3.182	−0.455	2622	−931	−0.262		2.044	−3.134	−1.534	0.772
	H···N	1.845	0.230			645			−14.76	0.276	−0.052	−0.190	0.353
NO1	N–H	1.014	6.866	−0.227	−0.032	3521	−32	−0.009		2.318	−3.433	−1.481	0.909
	H···O	2.166	0.091			405			−3.17	0.099	0.016	0.162	0.273
NO2	N–H	1.015	6.856	−0.136	−0.019	3518	−35	−0.010		2.317	−3.433	−1.482	0.908
	H···O	2.153	0.109			442			−3.25	0.104	0.015	0.143	0.231
NO3	N–H	1.014	6.853	−0.139	−0.020	3517	−36	−0.010		2.318	−3.405	−1.469	0.906
	H···O	2.317	0.050			298			−3.64	0.081	0.013	0.162	0.231
NO4	N–H	1.015	6.813	−0.179	−0.026	3507	−46	−0.013		2.314	−3.413	−1.475	0.907
	H···O	2.250	0.064			337			−3.77	0.093	0.014	0.146	0.248
NO5	N–H	1.016	6.765	−0.227	−0.032	3495	−58	−0.016		2.307	−3.420	−1.483	0.905
	H···O	2.192	0.090			402			−4.48	0.106	0.014	0.131	0.272
NO6	N–H	1.009	7.101	−0.517	−0.068	3580	−128	−0.035		2.333	−3.807	−1.632	0.917
	H···O	2.002	0.142			504			−5.12	0.146	0.008	0.057	0.326
NO7	N–H	1.011	6.951	−0.578	−0.077	3542	−145	−0.039		2.327	−3.825	−1.644	0.912
	H···O	1.959	0.172			554			−5.94	0.161	0.005	0.032	0.326
NO8	N–H	1.014	6.938	−0.054	−0.008	3539	−14	−0.004		2.323	−3.472	−1.495	0.911
	H···O	2.529	0.047			289			−12.90	–	–	–	0.227
NS1	N–H	1.014	6.812	−0.180	−0.026	3507	−46	−0.013		2.318	−3.381	−1.459	0.906
	H···S	2.810	0.027			215			−2.99	0.060	0.006	0.100	0.194
NS2	N–H	1.015	6.756	−0.236	−0.034	3492	−61	−0.017		2.312	−3.379	−1.462	0.905
	H···S	2.700	0.052			301			−3.76	0.075	0.006	0.078	0.234
NS3	N–H	1.014	6.839	−0.153	−0.022	3514	−39	−0.011		2.319	−3.381	−1.458	0.907
	H···S	2.886	0.030			229			−3.79	0.053	0.006	0.113	0.201
NF1	N–H	1.011	7.006	0.014	0.002	3556	3	0.001		2.338	−3.373	−1.443	0.914
	H···F	2.826	0.007			110			−1.42	0.017	0.005	0.285	0.134
NF2	N–H	1.013	6.946	−0.046	−0.007	3541	−12	−0.003		2.329	−3.402	−1.461	0.912
	H···F	2.355	0.028			224			−2.69	0.061	0.011	0.174	0.197
NF3	N–H	1.012	6.990	−0.002	0.0003	3552	−1	0.000		2.335	−3.387	−1.451	0.913
	H···F	2.494	0.035			250			−1.05	0.043	0.008	0.178	0.254
NCl1	N–H	1.012	6.972	−0.020	−0.003	3548	−5	−0.001		2.332	−3.365	−1.443	0.913
	H···Cl	2.968	0.030			227			−0.50	0.032	0.006	0.198	0.201
NCl2	N–H	1.013	6.926	−0.066	−0.009	3536	−17	−0.005		2.327	−3.386	−1.455	0.911
	H···Cl	2.867	0.022			196			−3.16	0.045	0.007	0.160	0.184
ON1	O–H	0.972	7.244	−1.311	−0.153	3601	−312	−0.080		2.401	−4.971	−2.070	0.923
	H···N	1.955	0.198			598			−6.83	0.206	−0.024	−0.117	0.339
ON2	O–H	0.975	6.956	−1.599	−0.187	3529	−384	−0.098		2.380	−4.921	−2.068	0.912
	H···N	1.915	0.216			625			−7.67	0.231	−0.036	−0.154	0.347
ON3	O–H	0.973	7.188	−1.367	−0.160	3587	−326	−0.083		2.399	−4.982	−2.077	0.921
	H···N	1.924	0.201			602			−7.71	0.213	−0.026	−0.121	0.341
ON4	O–H	1.000	4.972	−3.050	−0.436	2984	−806	−0.213		2.194	−4.526	−2.063	0.831
	H···N	1.751	0.290			724			−12.90	0.332	−0.092	−0.278	0.377
OO1	O–H	0.966	7.860	−0.695	−0.081	3751	−162	−0.041		2.455	−5.077	−2.068	0.944
	H···O	1.937	0.174			557			−4.98	0.175	−0.005	−0.027	0.327
OO2	O–H	0.967	7.690	−0.865	−0.101	3710	−203	−0.052		2.443	−5.056	−2.069	0.938
	H···O	1.898	0.172			555			−5.58	0.195	−0.012	−0.062	0.326
OO3	O–H	0.968	7.614	−0.941	−0.110	3692	−221	−0.056		2.439	−5.048	−2.070	0.935
	H···O	1.876	0.179			567			−5.75	0.206	−0.017	−0.082	0.330
OO4	O–H	0.966	7.870	−0.685	−0.080	3754	−159	−0.041		2.460	−5.072	−2.062	0.944
	H···O	1.972	0.144			507			−4.96	0.164	0.003	0.016	0.310
OO5	O–H	0.967	7.723	−0.832	−0.097	3718	−195	−0.050		2.445	−5.049	−2.065	0.939
	H···O	1.928	0.171			553			−5.62	0.182	−0.005	−0.027	0.326
OO6	O–H	0.970	7.484	−1.071	−0.125	3660	−253	−0.065		2.425	−5.016	−2.069	0.931
	H···O	1.886	0.175			559			−6.70	0.201	−0.012	−0.059	0.328

(continued)

Table 1. (Continued)

Molecule	Bond	R	k_a	Δk_a	$\Delta k_a/k_a$	ω_a	$\Delta\omega_a$	$\Delta\omega_a/\omega_a$	ΔE	ρ_c	H_c	H_c/ρ_c	n
OO7	O–H	0.964	7.934	−0.615	−0.072	3769	−143	−0.037		2.490	−5.147	−2.067	0.946
	H···O	1.933	0.181			569			−5.00	0.178	−0.006	−0.031	0.331
OO8	O–H	1.086	0.861	−7.694	−0.899	1241	−2672	−0.683		1.668	−2.954	−1.771	0.510
	H···O	1.408	0.217			623			−34.57	0.686	−0.383	−0.558	0.348
OO9	O–H	0.985	6.217	−1.805	−0.225	3336	−454	−0.120		2.311	−4.814	−2.083	0.884
	H···O	1.786	0.206			608			−10.85	0.256	−0.035	−0.137	0.343
OO10	O–H	0.969	7.459	−1.096	−0.128	3654	−259	−0.066		2.430	−5.043	−2.075	0.931
	H···O	2.027	0.089			398			−10.85	0.152	0.013	0.086	0.271
OS1	O–H	0.963	8.056	−0.499	−0.058	3798	−115	−0.029		2.484	−5.091	−2.049	0.950
	H···S	2.531	0.078			368			−2.86	0.099	0.001	0.011	0.262
OS2	O–H	0.965	7.859	−0.696	−0.081	3751	−162	−0.041		2.466	−5.057	−2.051	0.944
	H···S	2.453	0.104			425			−4.19	0.118	−0.002	−0.015	0.284
OS3	O–H	0.967	7.657	−0.898	−0.105	3702	−211	−0.054		2.449	−5.021	−2.050	0.937
	H···S	2.392	0.125			465			−5.23	0.136	−0.006	−0.045	0.298
OS4	O–H	0.965	7.875	−0.680	−0.079	3755	−158	−0.040		2.470	−5.059	−2.049	0.944
	H···S	2.505	0.077			365			−4.35	0.106	0.002	0.015	0.261
OS5	O–H	0.966	7.782	−0.773	−0.090	3732	−181	−0.046		2.460	−5.044	−2.050	0.941
	H···S	2.471	0.092			401			−4.83	0.114	0.000	−0.002	0.274
OS6	O–H	0.967	7.654	−0.901	−0.105	3702	−211	−0.054		2.445	−5.019	−2.053	0.937
	H···S	2.440	0.107			431			−6.00	0.122	−0.002	−0.014	0.286
OF1	O–H	0.957	8.530	−0.025	−0.003	3908	−5	−0.001		2.535	−5.157	−2.035	0.965
	H···F	2.569	0.008			116			−0.35	0.028	0.007	0.249	0.139
OF2	O–H	0.961	8.252	−0.303	−0.035	3844	−69	−0.018		2.495	−5.133	−2.057	0.957
	H···F	2.009	0.110			442			−3.41	0.121	0.014	0.118	0.288
OF3	O–H	0.959	8.398	−0.157	−0.018	3877	−36	−0.009		2.519	−5.153	−2.045	0.961
	H···F	2.182	0.029			226			−1.41	0.078	0.012	0.161	0.199
FO1	F–H	0.939	7.618	−2.101	−0.216	3676	−475	−0.114		2.353	−5.581	−2.371	0.936
	H···O	1.697	0.319			756			−9.22	0.299	−0.066	−0.220	0.387
FN1	F–H	0.956	5.964	−3.755	−0.386	3252	−900	−0.217		2.213	−5.073	−2.292	0.874
	H···N	1.679	0.375			823			−14.18	0.382	−0.128	−0.336	0.405
FF1	F–H	0.921	9.480	−0.803	−0.083	4100	−52	−0.012		2.517	−5.955	−2.366	0.994
	H···F	1.811	0.168			546			−4.37	0.184	−0.004	−0.021	0.324
FF2	F···H	1.145	0.803	−8.916	−0.917	1194	−2957	−0.712	−43.20	1.211	−1.684	−1.390	0.5
OCl1	O–H	0.961	8.172	−0.383	−0.045	3825	−88	−0.022		2.496	−5.113	−2.049	0.954
	H···Cl	2.510	0.051			297			−3.27	0.085	0.008	0.094	0.233
OCl2	O–H	0.958	8.465	−0.090	−0.011	3893	−20	−0.005		2.525	−5.139	−2.035	0.963
	H···Cl	2.815	0.029			223			−1.17	0.046	0.007	0.149	0.199
ClO1	Cl–H	1.303	3.999	−1.138	−0.222	2632	−351	−0.118		1.609	−1.608	−1.000	0.782
	H···O	1.853	0.167			546			−5.81	0.222	−0.015	−0.069	0.323
ClN1	Cl–H	1.341	2.268	−2.869	−0.558	1982	−1001	−0.336		1.457	−1.403	−0.963	0.668
	H···N	1.729	0.183			575			−10.55	0.365	−0.109	−0.297	0.331
ClCl1	Cl–H	1.286	4.898	−0.239	−0.047	2913	−70	−0.024		1.676	−1.683	−1.004	0.831
	H···Cl	2.549	0.060			323			−1.75	0.083	0.007	0.084	0.243
ClCl2	Cl···H	1.565	0.225	−4.913	−0.956	625	−2358	−0.791	−23.24	0.825	−0.564	−0.684	0.351
SS1	S–H	1.462	0.622	−3.741	−0.857	1039	−1714	−0.623		1.155	−0.914	−0.792	0.474
	H···S	1.987	0.095			406			−17.31	0.358	−0.104	−0.290	0.277
PP1	P–H	1.445	2.385	−0.962	−0.287	2036	−377	−0.156		1.131	−1.158	−1.024	0.677
	H···P	2.678	0.064			334				0.110	−0.002	−0.014	0.248
FH	F–H	0.918	9.719			4152				2.557	−5.990	−2.342	1.0
ClH	Cl-H	1.280	5.138			2984				1.700	−1.714	−1.008	0.839
OH2	O–H	0.957	8.555			3913				2.536	−5.153	−2.032	0.996
NH3	N–H	1.011	6.992			3553				2.336	−3.365	−1.440	0.914
SH2	S–H	1.341	4.363			2753				1.482	−1.509	−1.018	0.810
PH3	P–H	1.418	3.347			2413				1.107	−1.098	−0.991	0.744
FAM	N–H	1.002	7.618			3708				2.383	−3.728	−1.565	0.936
TFAM	N–H	1.003	7.529			3687				2.384	−3.741	−1.569	0.932
IA	N–H	1.002	7.593			3702				2.393	−3.830	−1.601	0.934
FA	O–H	0.966	8.022			3790				2.479	−5.090	−2.053	0.949
ME	O–H	0.956	8.549			3912				2.564	−5.198	−2.027	0.966

FAM, formamide; TFAM, thioformamide; IA, imidazole; FA, formic acid; ME, methanol.

[a] Bond length values R in Å, force constant k_a in mdyn/Å, vibrational frequency ω_a in cm^{-1}, binding energy ΔE in kcal/mol, electron density ρ_c at the bond critical point in e/Å^3, energy density H_c at the bond critical point in Hartree/Å^3, energy density per electron $\kappa_c = H_c/\rho_c$ in Hartree.

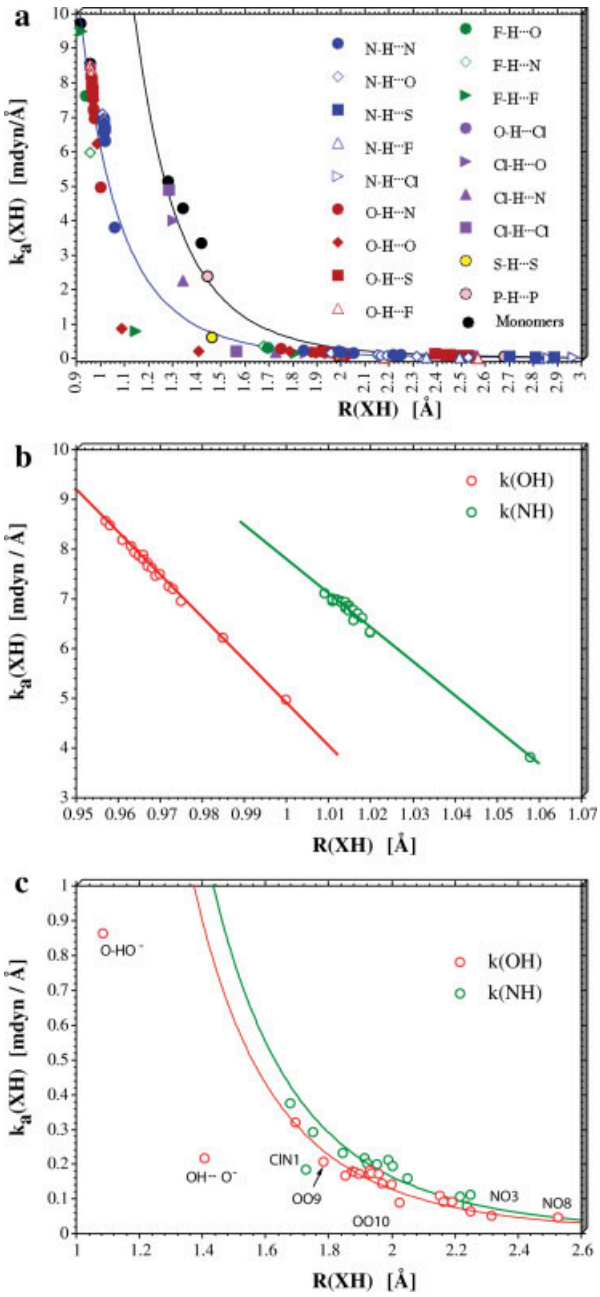

Figure 2. a) Local mode stretching force constants k_a in mdyn/Å are given for the (donor-hydrogen) DH bonds and H-bonds HA of the complexes shown in Figure 1 in dependence of the corresponding interaction distances R in Å. ωB97X-D/aug-cc-pVTZ calculations. b) Singling out covalent N–H and O–H bonds. c) Singling out $H\cdots N$ and $H\cdots O$ hydrogen bonds. [Color figure can be viewed in the online issue, which is available at wileyonlinelibrary.com.]

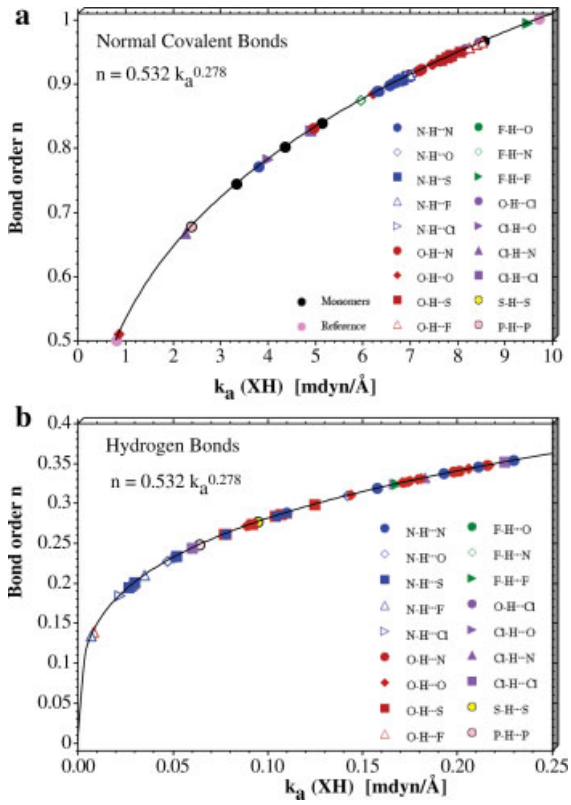

Figure 3. Bond order n given as a function of the local mode stretching force constants k_a as calculated for a) covalent DH bonds and b) hydrogen bonds of predominantly covalent or electrostatic nature. ωB97X-D/aug-cc-pVTZ calculations. [Color figure can be viewed in the online issue, which is available at wileyonlinelibrary.com.]

stretching force constants are relatively small, which indicates that the semiquantitative character of Badger's rule does not lead to a reliable description of HB on the basis of calculated bond distance values R.

The strongest scattering of data points is found for the anionic systems with strong HB where the values of R are smaller than those suggested by the power relationship (Figs. 2a and 2c). This is a direct reflection of the fact that the distance R is an unreliable bond strength descriptor in the case of charged molecules or molecules with strong charge polarization. This becomes obvious for the covalent HBs in $(F\cdots H\cdots F)^-$ (**FF1**: R = 1.145 Å; k_a = 0.803 mdyn/Å). Because of the strong electronegativity of F the

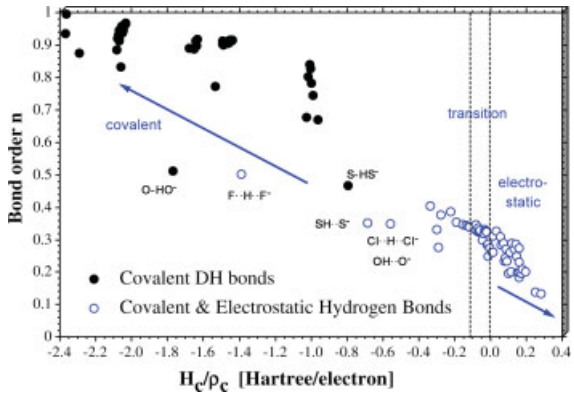

Figure 4. Comparison of the bond order n based on local mode stretching force constants k_a with the electron density-normalized energy density $\kappa_c = H_c/\rho_c$ at the bond critical point $\mathbf{r}_c$. Formal DH single bonds are given by filled black circles whereas hydrogen bonds are given by empty blue circles. Three bonding regions (covalent, transition, electrostatic) are indicated. For the notation of HB systems, see Figure 1; ωB97X-D/aug-cc-pVTZ calculations. [Color figure can be viewed in the online issue, which is available at wileyonlinelibrary.com.]

central H atom has lost most of its electron density and therefore has no longer the covalent bonding radius of the H atom in FH. Therefore, the distances between H and F atoms in **FF1** are strongly decreased and accordingly do not fulfill the exponential relationship shown in Figure 2a. Similar observations can be made for other ionic HB-systems (Fig. 1, see also Table 1), which are mainly responsible for the strong scattering of data points in Figure 2a.

The covalent radius of an atom and thereby also distance R depend on the number of core shells, the charge of the atom, electron spin arrangements, and enviromental factors influencing the bond density distribution. Attempts to derive effective bond lengths R_{eff} as first done by Badger[95] may lead to some limited improvement when using R as a bond strength descriptor in the case of covalent XY bonds (for example, the NH and OH bonds investigated in this work; see Fig. 2b), but in the case of larger variations in atom,atom distances $R(HA)$ leading to small changes in the local mode stretching force constants, the Badger rule is poised to fail and interaction distances R can no longer be considered as reliable bond strength descriptors.

Electron density and the Laplacian of the density at the bond critical point $\mathbf{r}_c$ between atoms H and A have been used to assess the nature of HB.[41,47–51,96–100] Espinoza et al.[41,42] used in addition the energy density criterion derived by Cremer and Kraka[38–40] for distinguishing between covalent and electrostatic HBs. Despite the usefulness of these descriptions, single density values cannot reflect integral density properties associated with the whole bond region. Cremer and Gauss[101] have related the electron density obtained by integration over the zero-flux surface between two neighboring virial (atomic) spaces to the bond strength and they could reproduce trends in CC and CH bond energies for alkanes and cycloalkanes. However, these authors have also emphasized that the zero-flux density only reflects trends in covalent bond strengths whereas the ionic (polar) character of a bond can only be assessed from a quantitative description of the density polarization in the bond region. Currently, there is no electron density or energy density based quantity that can be used as a reliable indicator of the intrinsic HB strength.

BSSE-corrected binding energies $\Delta E = E(\text{complex}) - E(\text{monomer 1}) - E(\text{monomer 2})$ are normally used to describe the strength of HB. We emphasize that these values do not correspond to the intrinsic strength of the HB. When breaking the latter the bond DH relaxes to its normal length as does the electron density distribution of this bond and other bonds connected to donor D and/or acceptor A where especially the electron density in the lone pair region of A relaxes. Geometry and electron density relaxation of DH and A lead to their stabilization (stabilization energy SE) and by this to a significant decrease in the binding energy ΔE. SE values will vary with the electronic nature of D and A so that their effects on ΔE are difficult to predict. We define as the intrinsic HB binding energy $\Delta E(\text{intrinsic})$ that energy, which would result if both D and A after DHA dissociation remain in the geometry of the DHA complex and the electron density frozen in the distribution of the complex. The latter requirement is difficult to fulfill and accordingly none of the HB binding energies given in the literature or in this work fulfills the criteria of a true intrinsic binding energy $\Delta E(\text{intrinsic})$, which correctly reflects the strength of the HB. Hence, a true descriptor of the HB is only provided by the local mode HA stretching force constants $k_a(HA)$ given in this work (see Table 1).

Determination of H-bond orders

For the determination of a HB bond order, we assume that there is a continuous transition from electrostatic to covalent HB. Parallel to this change, there is a reverse change in the nature of the DH bond, which is increasingly weakened with increasing HB strength. The local mode stretching force constants $k_a(\text{DH})$ and $k_a(\text{HA})$ are sensitive with regard to the total density distribution enveloping the three atoms involved in HB and thereby they reflect all electrostatic and covalent contributions to HB, i.e., they present a measure of the intrinsic bond strength of both DH and HA interactions. We will exploit this fact by deriving a suitable HB strength descriptor in form of an HB bond order $n(XH)$ ($X = D$ or A), which can be easily used for the comparison of different DH and HA interactions in HB complexes.

In view of the continuous change in k_a values for a transition from covalent to ionic XH bonds observed by KLC,[14] it is reasonable to assume that a single relationship $n = f(k_a)$ is sufficient to describe the XH bonds investigated in this work. Any bond order relationship requires suitable reference values and a suitable mathematical function to map force constants onto bond orders. In recent work, it has been shown that the bond order n and the local mode stretching force constant k_a are connected by a power relationship.[13,14] The results obtained in this work suggest the extension of this relationship to non-covalent bonding. In this connection, it is necessary to require that a force constant equal to zero implies a bond order of zero, which makes sure that negative bond orders cannot occur. As reference for a DH single bond with bond order $n = 1$, we take the monomer FH, which has a bond dissociation energy (BDE) of 136.2 kcal/mol.[102] As a second reference system, we use the complex **FF2**, for which covalent bonding is established by the delocalization of four electrons in an all-bonding and a nonbonding MO. Hence, the bond order of **FF2** can be set to $2/(2 \times 2) = 0.5$.

In Figure 3, the power relationship between bond order n and local mode stretching force constant k_a obtained in this way (see also Table 1), is depicted where the covalent DH bonds are shown in Figure 3a and the HBs in Figure 3b. By setting the bond order of the FH bond to 1, the bond orders of all OH or NH bonds become smaller than 1, which is reasonable in view of the fact that the corresponding BDE values (OH_2: 118.8 kcal/mol; NH_3: 107.6 kcal/mol[102]) are smaller than the value of BDE(FH). One can scale the OH, NH or other interactions with D and A $\neq$ F by resetting n(OH), n(NH), etc. for OH_2, NH_3, etc. equal to 1. However in this work, we refrain from using other references. The bond order n is used here to compare all HBs of the complexes and monomers in Figure 1.

In Figure 4, calculated bond orders are compared with the bond index $\kappa_c = H_c/\rho_c$. As expected, there is no direct relationship between n, which represents the total electron density in the

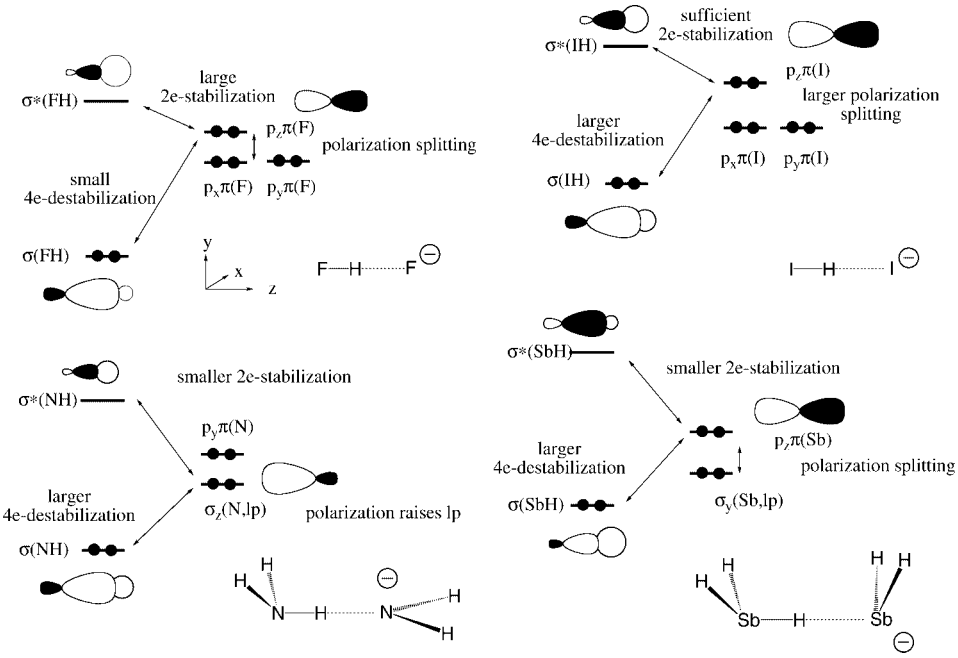

Figure 5. PMO analysis of charge assisted hydrogen bonding. Orbital interactions are shown after mutual polarization before the formation of the final MOs. Upper left corner, $F\cdots H\cdots F^-$: 2e-delocalization is large and leads to a symmetric 3c-4e bonding situation. Upper right corner, $I\cdots H\cdots I^-$: Although 2e-delocalization should be smaller because of the lower electronegativity of I (leading to an energy increase in the $\sigma(IH)$ and $\sigma^\star(IH)$ orbital energies), the polarization splitting of the I^- orbitals helps to increase 2e-delocalization and to re-establish the symmetric 3c-4e bonding situation. Lower left corner, $H_2N–H\cdots NH_2^-$: 2e-delocalization is decreased and polarization effects are not sufficient to counterbalance this effect. An asymmetric 3c-4e bonding situation results. Lower right corner, $H_2Sb–H\cdots SbH_2^-$: To compensate the loss in 2e-stabilization caused by reduced electronegativity, the anion interacts via its pπ orbital. A new complex geometry leads to some weak, predominantly electrostatic interactions (see text).

interaction region, and the bond index κ_c obtained at a single point. There are a dozen HBs (open circles) in the covalent region, i.e., their κ_c value is smaller than −0.1 whereas most of the HBs investigated are in the electrostatic region with positive κ_c values or in a transition region between dominant covalent and dominant electrostatic HBs (Fig. 4).

Among the covalent HBs with bond orders between 0.28 and 0.5, there are especially the charge assisted HBs of **FF2**, **OO8**, **NN7**, **ClCl2**, or **SS1**. According to the pK_a or PA equilibration principle,[30, 56] these ions should have the H atom in a central position, equal negative charge at the heavy atoms, and D and A should attract the positively charged H atom with the same strength (i.e., D after loosing H as a proton and A have the same PA or pK_a values). The symmetrical double-well potential for proton transfer from D to A is replaced by a broad single-well potential. However, it is well-known that this situation is only fulfilled for the halogen anionic systems[28, 103] whereas for the O, N, S, P, and other anionic systems a double-well potential with low barrier is observed.[63, 64, 104–110]

The charge assisted HB have been frequently discussed and multiple attempts have been made to explain the large variation in their binding energies, the symmetric or asymmetric position of H, the differences in positive and negative charged ions or the shape of the PES for the proton transfer.[28, 103, 105–109] We note that in view of the covalent character of the charge assisted HBs (see Table 1 and Fig. 4) a simple MO explanation should be sufficient to explain the trends in calculated bond orders.

According to PMO theory, the interaction between the $\sigma(XH)$, $\sigma^\star(XH)$, and the pπ(X) (X = halogen) starting orbitals will depend on the electronegativity of X, the corresponding orbital energy differences $\Delta\epsilon$, and the overlap between the orbitals. A large electronegativity of X, leads to more negative orbital energies for $\sigma(XH)$ and $\sigma^\star(XH)$, a larger $\Delta\epsilon(\sigma,\pi_z)$, which is even increased by the polarization of the $p_z\pi(X)$ orbital caused by exchange repulsion with the XH bond. The difference $\Delta\epsilon(\pi_z,\sigma^\star)$ is small and accordingly the 2e-stabilization (delocalization of the $p_z\pi(X)$ electron pair into the $\sigma^\star(XH)$ orbital) large whereas the 4e-destabilization is small (large $\Delta\epsilon(\sigma,\pi_z)$). This leads to a delocalized, strongly stabilized 3c-4e system and a symmetric position of the H atom as in the case X = F (Table 1).

With increasing atomic number of X, the electronegativity of X decreases and the $\sigma(XH)$ and $\sigma^\star(XH)$ orbitals are higher in energy. This would lead to a reduction of 2e-delocalization, an increase of 4e-destabilization, and a shift of the H toward the D atom (asymmetric DHA configuration). However, the polarization splitting of the $p\pi(X)$ orbitals (Fig. 5) is now larger due to the larger polarizability of X and its diffuse electron lone pairs. Hence the situation of X = F can be regained (central position of H atom) despite the lower electronegativity of X.

The situation will be different if X corresponds to a group such as OH, NH_2, SH, or PH_2. Polarization splitting cannot push the $\sigma_z(X)$ lone pair energy above that of the $p_x\pi(X)$ lone pair, which means that the decrease in electronegativity (increase in 4e-destabilization, decrease of 2e-stabilization) enforces an

asymmetric DHA configuration and a (small) barrier to proton transfer as found for X = OH.[104] A weaker HB is obtained as reflected by the calculated binding energies ΔE of 34.6 and 14.8 kcal/mol for **OO8** and **NN7** (Table 1).

For third period systems with X = SH and PH_2, the binding energy is reduced to 17.3 and 5.6 kcal/mol, respectively (**SS1** and **PP1**, Table 1) compared to the corresponding **ClCl2** value of 23.2 kcal/mol. Obviously, charge assistance does no longer play a role for **PP1** in view of the low electronegativity of P. However, the **PP1** complex can gain some stabilization by a 90° rotation of the PH_2 anion, which makes the use of the better polarizable $p\pi(P)$ orbital possible and thereby causes a somewhat better 2e-stabilization energy. It is interesting to note that **PP1** prefers a semieclipsed conformation, which leads to slightly better electrostatic interactions (involving the bond and lone pair dipole moments). The trends observed in this work for X = Cl, SH, and PH_2, we have also found for X = Br, SeH, and AsH_2 as well as I, TeH, and SbH_2 (not reported in Table 1).

Noteworthy is that the calculated (and experimental) ΔE value for **FF2** is 43.2 (exp $\Delta H(298)$: 45.8 kcal/mol[102]), which is lower than half of the BDE of FH (136.2 kcal/mol[102]). This reflects the stabilization energies of the fragments FH and F^- and confirms the large changes in calculated binding energies upon geometry and density relaxation as discussed above.

If D is strongly electronegative as in FH and A has an polarizable electron pair as in NH_3 a significantly covalent HB is obtained as is indicated by the increase in bond orders (and binding energies) in the series **FF1**, **FO1**, and **FN1** (Table 1: 0.324, 0.387, 0.405; ΔE: 4.4, 9.1, 14.8 kcal/mol). In these HB systems, delocalization into the $\sigma^*(FH)$ bond is facilitated and at the same time the electrostatic interactions between H and A are increased due to the electronegativity of the F atom.

Noteworthy is also the strong HB involving the NH_2 group of amides such as **NN3**, **NN4**, **NO6**, or **NO7** with bond orders of 0.318, 0.337, 0.326, and 0.326 (6.90, 8.05, 5.12, 5.94 kcal/mol, Table 1), which all belong to the class of resonance assisted HBs[111] as does **NN6** involving the NH group of imidazole (Fig. 1). In a resonance assisted HB systems, π-delocalization leads to a larger polarity of the NH bond and an increase of both covalent and electrostatic contributions to the HB. A similar situation is found for ring systems such as **NO8** or **ON4**, which benefit from two HBs (Fig. 1).

The weakest HB is found for **NF1** or **OF1**, which involve the poorly polarizable F_2 molecule and therefore yield only bond orders of 0.134 and 0.139 and κ_c values larger than 0.2 (Table 1). This is typical of weak, exclusively electrostatic (noncovalent) interactions.

Bond orders and binding energies of HB

In Figure 6a, BSSE-corrected HB binding energies are related to calculated HB bond orders $n(HA)$. There is a strong scattering of ΔE values, which makes it difficult to extract even a qualitative relationship between these quantities. The HB binding energy ΔE includes energy effects caused by a new interaction HA and the weakening of the existing DH bond. Hence, ΔE should be related to the sum of changes in the bond orders rather than

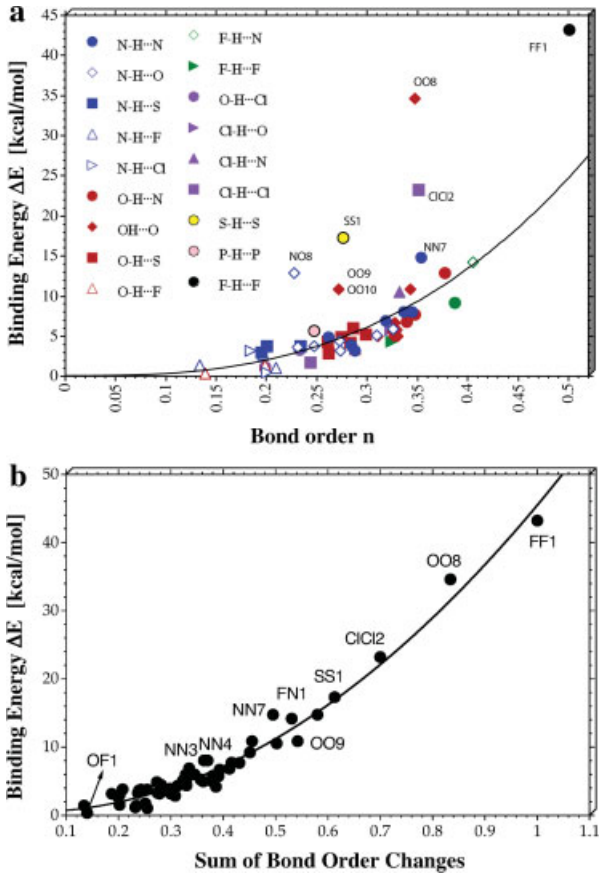

Figure 6. HB binding energy ΔE given as a function of a) calculated bond orders $n(HA)$ and b) the sum of bond order changes caused by complex formation due to hydrogen bonding. ωB97X-D/aug-cc-pVTZ calculations. [Color figure can be viewed in the online issue, which is available at wileyonlinelibrary.com.]

a single bond order $n(HA)$. The change in the DH bond can be assessed by subtracting the bond order for the monomer DH from that in the complex whereas the bond order of HA can be directly taken from Table 1.

In Figure 6b, ΔE values are given in dependence of the sum of bond order changes $\Delta n(DH) + n(HA)$. Although there is still some scattering of values, the binding energy ΔE has a quadratic dependence on the sum of bond orders (R^2 = 0.969), which confirms that local mode force constants provide a measure of the HB strength. Because the binding energy also includes other geometry and electron density relaxation effects upon HB dissociation, an exact relationship cannot be expected. Nevertheless, the strong binding in the case of charge assisted HB and other covalent HBs becomes obvious from Figure 6b.

Vibrational spectroscopy as a tool for describing H-bonding

In Table 1, the local mode frequencies of the HB are listed together with their associated stretching force constants. They reach from about 100 to 800 cm^{-1} with the exception of **FF2**, which has a HF stretching frequency of 1194 cm^{-1}. Accordingly, local mode stretching force constants vary from 0.03 to 0.8 mdyn/Å. It has to be noted that changes in the frequencies larger than 5 cm^{-1}

(3×10^{-3} mdyn/Å) are relevant, which is the reason why bond orders are given with an accuracy of 10^{-3}.

Calculated red shifts $\Delta\omega_a(DH)$ and normalized red shifts $\eta(DH)$ for DH bonding are listed in Table 1. In Figure 7, the latter are related to the local HA stretching frequencies. As in the case of the binding energies and bond orders, Figure 7 confirms that the description of HB exclusively via the red shifts of the DH stretching frequencies can be useful only in the case of closely related HBs (e.g., HB in water complexes[23]). It can be strongly misleading if different HBs are investigated as is revealed by the strong scattering of results for charge-assisted HBs. This scattering does not change when $\Delta\omega_a(DH)$ rather than $\eta(DH)$ (Fig. 7a) is used. Clearly, frequencies are quantities, which, because of their mass dependence, should not be used to describe the strength of a bond. Experimentally, however they are exclusively available whereas the corresponding force constants have to be calculated.

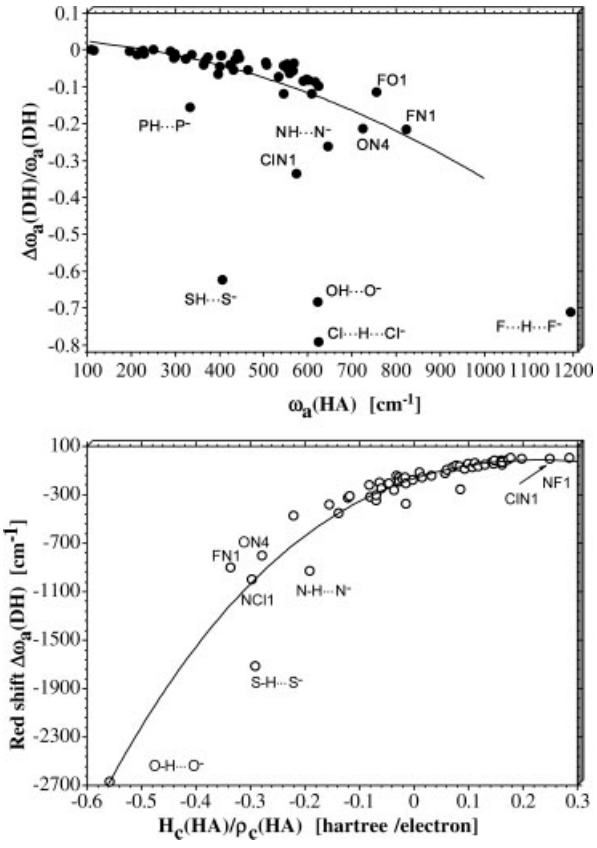

Figure 7. a) Calculated normalized red shifts $\eta_a(DH) = \Delta\omega_a(DH)/\omega_a(DH)$ based on local mode frequencies given as a function of local mode HA stretching frequencies $\omega_a(HA)$. b) Calculated red shifts $\Delta\omega_a(DH)$ given as a function of normalized energy densities $\kappa_c(HA) = H_c(HA)/\rho_c(HA)$. ωB97X-D/aug-cc-pVTZ calculations.

The local mode force constants do not suffer from coordinate dependence or other deficiencies and in addition can be derived from experimental frequencies.[11] Nevertheless, the general message of Figure 7 does not change if $\Delta k_a(DH)/k_a(DH)$ is related to $k_a(HA)$ values. Any combination of bond order, frequency, force constant, energy density, or electron density values calculated for DH and HA does not lead to a reasonable correlation as long as not all changes in the complex due to HB are included.

From a qualitative point of view, the normalized frequency shifts η are useful parameters for distinguishing weak HBs ($0 > \eta > -0.1$) from more covalent and stronger HBs ($\eta < -0.1$) where the negative sign is due to the red shift. Test calculations show that η becomes positive for blue shifted HB as they occur when π-systems are involved.

Conclusions

Local vibrational modes provide a sensitive tool to detect and characterize HB in complexes DHA. For this purpose, the local stretching force constants of both the DH and HA bond have to be determined. The stretching force constants register all changes in the electron density distribution between donor D and acceptor A. They provide a global rather than a local measure of bonding, the latter of which is used when the electron or energy density distribution is analyzed at the bond critical point. The vibrational analysis based on local modes and carried out in this work reflects the total bond strength and therefore provides important insights into HB:

1. Local mode stretching force constants can be used to order HBs according to their strength. In this work, FH and the anion **FF2** typical of charge-assisted HB are selected to obtain suitable reference bond orders of $n = 1$ and $n = 0.5$ and to derive a power relationship between local mode stretching force constant k_a and bond order n. We note that if the choice of the reference bond orders is done differently, different bond orders will result, however the relative ordering of HBs according to their strength will not change.

2. By combining the bond orders derived from local mode properties with the Cremer-Kraka criterion of covalent bonding based on the energy density at the bond critical point,[38–40] HBs with dominant covalent character can be distinguished from HBs with dominant electrostatic character.

3. When comparing the HB orders obtained in this work with bond distances, density properties, or HB binding energies, the deficiencies of the latter properties as possible bond strength descriptors become obvious. Electron and energy densities do not provide reliable bond descriptors as long as they are calculated at single points in the bond region rather than being integrated over the whole bond region. However, a quantum mechanical definition of the bond region does not exist. Similarly, bond distances can only function as bond strength descriptors if they can be transformed into an effective bond distance eliminating the influence of core shells, atomic charges, electron spin, or bond bending. There is no general way of obtaining such effective bond lengths. Finally, HB binding energies are depending on both the HB strength and the stabilization energies of the separated monomers, which makes them unsuitable as bond strength descriptors.

4. For the purpose of quantitatively assessing the strength of a HB both the change in the DH bond order and the n value of the newly generated HA bond has to be considered. If this is done, HB binding energies correlate with bond orders ($R^2 = 0.969$) for

a large variety of HBs involving charged assisted covalent HBs with D and A from either the second or the third period, weak electrostatic HB, resonance assisted HBs, or double HBs in cyclic systems. The remaining scattering of data points reflects the shortcomings of binding energies as bond strength descriptors.

5. Local vibrational modes and their properties provide a generally applicable tool for describing weak interactions such as HBs. This tool will work with any quantum chemical method nowadays available to calculate normal mode frequencies. In this work, we have used DFT and the ωB97X-D functional in connection with the aug-cc-pVTZ basis set, which is known to lead to HB results close to those obtained with CCSD(T).[84]

6. It is important to note that the local modes obtained in this work by solving the basic equations of vibrational spectroscopy, can also be determined once the experimental vibrational frequencies of a molecule or complex are known. In this way, the local mode approach of Konkoli and Cremer[8] represents a new dimension of describing HB or weak noncovalent interactions in general. Of course, for most HB complexes it is unlikely that all 3K-L vibrational frequencies can be accurately measured. However, there are procedures that help to complement measured vibrational frequencies to a complete set utilizing either scaled harmonic or anharmonically corrected quantum chemical frequencies thus opening a wide range of application possibilities for the use of local mode properties.

Acknowledgments

The authors thank SMU for providing computational resources.

Keywords: hydrogen bonding • local vibrational modes • hydrogen bond stretching force constants • strength of the hydrogen bond • hydrogen bond order

How to cite this article: M. Freindorf, E. Kraka, and D. Cremer, *Int. J. Quantum Chem.* **2012**, DOI: 10.1002/qua.24118

[1] D. McKean, *Spectrochim. Acta A* **1975**, *31*, 1167.
[2] D. McKean, *Chem. Soc. Rev.* **1978**, *7*, 399.
[3] D. McKean, *Int. J. Chem. Kinet.* **1989**, *21*, 445.
[4] W. F. Murphy, F. Zerbetto, J. L. Duncan, D. McKean, *J. Phys. Chem.* **1993**, *97*, 581.
[5] B. Henry, *Acc. Chem. Res.* **1987**, *20*, 429.
[6] G. Sbrana, M. Muniz-Miranda, *J. Phys. Chem. A* **1998**, *102*, 7603.
[7] M. Hippler, M. Quack, *Ber. Busenges. Phys. Chem.* **1997**, *101*, 356.
[8] Z. Konkoli, D. Cremer, *Int. J. Quant. Chem.* **1998**, *67*, 1.
[9] Z. Konkoli, D. Cremer, *Int. J. Quant. Chem.* **1998** *67*, 29.
[10] J. Larsson, D. Cremer, *J. Mol. Struct.* **1999**, *67*, 385.
[11] D. Cremer, J. Larsson, Kraka, In Theoretical and Computational Chemistry, Vol. 5, Theoretical Organic Chemistry, C. Parkanyi, Ed.; Elsevier: Amsterdam, **1998**; p. 259.
[12] J. Oomens, E. Kraka, M. Nguyen, T. Morton, *J. Phys. Chem. A* **2008**, *112*, 10774.
[13] E. Kraka, D. Cremer, *Chem. Phys. Chem.* **2009**, *10*, 686.
[14] E. Kraka, J. Larsson, D. Cremer, In Vibrational Modes in Computational IR Spectroscopy; J. Grunenberg, Ed.; Wiley: New York, **2010**; p. 105.
[15] D. Cremer, E. Kraka, *Curr. Org. Chem.* **2010**, *14*, 1524.
[16] W. Zou, R. Kalescky, E. Kraka, D. Cremer, *J. Phys. Chem.* **2012**, submitted.
[17] E. Kraka, D. Cremer, *Acc. Chem. Res.* **2010**, *43*, 591.
[18] E. Kraka, In Wiley Interdisciplinary Reviews: Computational Molecular Science, Reaction Path Hamiltonian and the Unified Reaction Valley Approach, W. Allen, P. R. Schreiner, Eds.; Wiley: New York, **2011**; p. 285.
[19] G. Jeffrey, An Introduction to Hydrogen Bonding; Oxford University Press: New York, **1997**.
[20] G. Jeffrey, W. Saenger, Hydrogen Bonding in Biological Structures; Springer-Verlag: Berlin, **1991**.
[21] S. Scheiner, Hydrogen Bonding: A Theoretical Perspective; Oxford University Press: New York, **1997**.
[22] P. E. Pihko, Hydrogen Bonding in Organic Synthesis; Wiley: New York, **2009**.
[23] S. J. Grabowski, Ed., Hydrogen Bonding—New Insights, in Challenges and Advances in Computational Chemistry and Physics; Vol. 3, J. Leszczynski, Series Ed., Springer, New York, **2006**.
[24] G. Gilli, P. Gilli, The Nature of the Hydrogen Bond- IUCr Monographs on Crystallography-23; Oxford University Press: New York, **2009**.
[25] K. Müller-Dethlefs, P. Hobza, *Chem. Rev.* **2000**, *100*, 143.
[26] T. Steiner, *Angew. Chem. Int. Ed.* **2002**, *41*, 48.
[27] N. Belkova, E. Shubina, L. M. Epstein, *Acc. Chem. Res.* **2005**, *38*, 624631.
[28] M. Meot-Ner, *Chem. Rev.* **2005**, *105*, 213.
[29] P. Munshi, T. Row, *Cryst. Rev.* **2005**, *11*, 199.
[30] P. Gilli, L. Pretto, V. Bertolasi, G. Gilli, *Acc. Chem. Res.* **2009**, *42*, 33.
[31] S. Grabowski, *Chem. Rev.* **2011**, *111*, 2597.
[32] S. J. Grabowski, W. A. Sokalski, *J. Phys. Org. Chem.* **2005**, *18*, 779.
[33] M. Ziolkowski, S. Grabowski, J. Leszcynski, *J. Phys. Chem.* **2006**, *110*, 6514.
[34] B. Skwara, A. Kaczmarek, R. W. Gora, W. Bartkowiak, *Chem. Phys. Lett.* **2008**, *461*, 203.
[35] R. Bader, Atoms in Molecules: A Quantum Theory; Oxford University Press: Oxford, **1990**.
[36] P. Popelier, Atoms in Molecules: An Introduction; Prentice Hall: London, **2000**.
[37] C. Matta, R. Boyd, The Quantum Theory of Atoms in Molecules: From Solid State to DNA and Drug Design; Wiley-VCH: Weinheim, **2007**.
[38] D. Cremer, E. Kraka, *Angew. Chem. Int. Ed. Engl.* **1984**, *23*, 627.
[39] D. Cremer, E. Kraka, *Croat. Chem. Acta* **1984**, *57*, 1259.
[40] E. Kraka, D. Cremer, In Theoretical Models of Chemical Bonding. The Concept of the Chemical Bond, Vol. 2; Z. Maksic; Springer Verlag: Heidelberg, Germany, **1990**; p. 453.
[41] E. Espinosa, I. Alkorta, J. Elguero, E. Molins, *J. Chem. Phys.* **2002**, *117*, 5529.
[42] I. Mata, E. Molins, I. Alkorta, E. Espinosa, *J. Phys. Chem. A* **2011**, *115*, 12561.
[43] A. Reed, L. Curtiss, F. Weinhold, *Chem. Rev.* **1988**, *88*, 899.
[44] F. Weinhold, C. R. Landis, Valency and Bonding: A Natural Bond Orbital Donor-Acceptor Perspective; Cambridge University Press, Cambridge, **2003**.
[45] A. Becke, K. Edgecombe, *J. Chem. Phys.* **1990**, *92*, 5397.
[46] A. Savin, O. Jepsen, J. Flad, O. K. Andersen, H. Preuss, H. G. von Schnering, *Angew. Chem, Int. Ed. Engl.* **1992**, *31*, 187.
[47] U. Koch, P. Popelier, *J. Phys. Chem.* **1995**, *99*, 9747.
[48] O. Knop, K. Rankin, R. Boyd, *J. Phys. Chem. A* **2001**, *105*, 6552.
[49] S. Grabowski, *J. Phys. Org. Chem.* **2004**, *17*, 18.
[50] I. Mata, I. Alkorta, E. Molins, E. Espinosa, *Chem. Eur. J.* **2010**, *16*, 2442.
[51] C. Gatti, P. Macchi, Modern Charge Density Analysis; Springer: New York, **2012**.
[52] F. Fuster, B. Silvi, *Theor. Chem. Acc.* **2000**, *104*, 13.
[53] F. Fuster, S. Grabowski, *J. Phys. Chem. A* **2011**, *115*, 10078.
[54] I. Mata, E. Molins, I. Alkorta, E. Espinosa, *J. Phys. Chem. A* **2007**, *111*, 6425.
[55] J. Conteras-Garcia, W. Yang, *J. Phys. Chem. A* **2011**, *115*, 12983.

[56] G. Gilli, P. Gilli, *J. Mol. Struct.* **2010**, *972*, 2.

[57] J. Dannenberg, L. Haskamp, A. Masunov, *J. Phys. Chem. A* **1999**, *103*, 7083.

[58] I. Mata, E. Molins, I. Alkorta, E. Espinosa, *J. Chem. Phys.* **2009**, *130*, 044104.

[59] H. Fliegel, O. Lehtonen, D. Sundholm, V. Kaila, *Phys. Chem. Chem. Phys.* **2011**, *13*, 434.

[60] C.-Y. Park, Y. Kim, Y. Kim, *J. Chem. Phys.* **2001**, *115*, 2926.

[61] B. Cherng, F.-M. Tao, *J. Chem. Phys.* **2001**, *114*, 1720.

[62] E. Nibbering, T. Elsaesser, *Chem. Rev.* **2004**, *104*, 1887.

[63] E. Diken, J. Headrick, J. Roscioli, J. Bopp, M. Johnson, A. McCoy, *J. Phys. Chem. A* **2005**, *109*, 1487.

[64] E. Diken, J. Headrick, J. Roscioli, J. Bopp, A. McCoy, X. Huang, S. Carter, J. Bowman, *J. Phys. Chem. A* **2005**, *109*, 517.

[65] C. Brindle, G. Chaban, R. Gerber, K. Janda, *Phys. Chem. Chem. Phys.* **2005**, *7*, 945.

[66] P. Janeiro-Barral, M. Mella, *J. Phys. Chem. A* **2006**, *110*, 11244.

[67] M. Slipchenko, B. Sartakov, A. Vilesov, S. Xantheas, *J. Phys. Chem. A* **2007**, *111*, 7460.

[68] T. Elsaesser, *Acc. Chem. Res.* **2009**, *42*, 1220.

[69] I. Heisler, S. Meech, *Science* **2010**, *327*, 857.

[70] X. Zhang, Y. Zeng, X. Li, L. Meng, S. Zgeng, *J. Mol. Struct. THEOCHEM*, **2010**, *7*, 27.

[71] X.-Z. Li, B. Walker, A. Michaelides, *PNAS* **2011**, *108*, 6369.

[72] N. de Lima, M. Ramos, *J. Mol. Struct.* **2011**, *7*, 29.

[73] S. Grabowski, *J. Phys. Chem. A* **2011**, *115*, 12789.

[74] R. Kalechvsky, E. Kraka, D. Cremer, *J. Phys. Chem.* **2012**, submitted.

[75] E. B. Wilson, J. C. Decius, P. C. Cross, Molecular Vibrations; McGraw-Hill Book Company: New York, **1955**.

[76] J. Decius, *J. Chem. Phys.* **1963**, *38*, 241.

[77] S. J. Cyvin, N. B. Slater, *Nature* **1960**, *188*, 485.

[78] S. J. Cyvin, In Molecular Vibrations and Mean Square Amplitudes; Universitetsforlaget, Oslo, **1971**, pp. 68–73.

[79] K. Brandhorst, J. Grunenberg, *Chem. Soc. Rev.* **2008**, *37*, 1558.

[80] J. Grunenberg, *J. Am. Chem. Soc.* **2004**.

[81] J. Baker, P. Pulay, *J. Am. Chem. Soc.* **2006**, *128*, 11324.

[82] X. Xu, W. A. Goddard, *J. Phys. Chem. A* **2004**, *108*, 2305.

[83] J. Anderson, G. Tschumper, *J. Phys. Chem. A* **2006**, *110*, 7268.

[84] K. Thanthiriwatte, E. Hohenstein, L. Burns, C. Sherrill, *J. Chem. Theor. Comp.* **2011**, *7*, 88.

[85] J.-D. Chai, M. Head-Gordon, *Phys. Chem. Chem. Phys.* **2008**, *10*, 6615.

[86] J.-D. Chai, M. Head-Gordon, *J. Chem. Phys.* **2008**, *128*, 084106.

[87] T. J. Dunning, *J. Chem. Phys.* **1989**, *90*, 1007.

[88] D. Woon, T. J. Dunning, *J. Chem. Phys.* **1993**, *98*, 1358.

[89] S. Boys, F. Bernardi, *Mol. Phys.* **1970**, *19*, 553.

[90] S. Simon, M. Duran, J. Dannenberg, *J. Chem. Phys.* **1996**, *105*, 11024.

[91] E. Kraka, J. Grafenstein, M. Filatov, A. Wu, H. Joo, D. Izotov, J. Gauss, Y. He, Z. He, V. Polo, F. Reichel, Z. Konkoli, L. Olsson, W. Zou, and D. Cremer, Southern Methodist University, Dallas, **2012**.

[92] Revision A.1, M. J. Frisch, G. W. Trucks, H. B. Schlegel, G. E. Scuseria, M. A. Robb, J. R. Cheeseman, G. Scalmani, V. Barone, B. Mennucci, G. A. Petersson, H. Nakatsuji, M. Caricato, X. Li, H. P. Hratchian, A. F. Izmaylov, J. Bloino, G. Zheng, J. L. Sonnenberg, M. Hada, M. Ehara, K. Toyota, R. Fukuda, J. Hasegawa, M. Ishida, T. Nakajima, Y. Honda, 0. Kitao, H. Nakai, T. Vreven, J. A. Montgomery, Jr., J. E. Peralta, F. Ogliaro, M. Bearpark, J. J. Heyd, E. Brothers, K. N. Kudin, V. N. Staroverov, R. Kobayashi, J. Normand, K. Raghavachari, A. Rendell, J. C. Burant, S. S. Iyengar, J. Tomasi, M. Cossi, N. Rega, J. M. Millam, M. Klene, J. E. Knox, J. B. Cross, V. Bakken, C. Adamo, J. Jaramillo, R. Gomperts, R. E. Stratmann, 0. Yazyev, A. J. Austin, R. Cammi, C. Pomelli, J. W. Ochterski, R. L. Martin, K. Morokuma, V. G. Zakrzewski, G. A. Voth, P. Salvador, J. J. Dannenberg, S. Dapprich, A. D. Daniels, Ö. Farkas, J. B. Foresman, J. V. Ortiz, J. Cioslowski, and D. J. Fox, Gaussian, Inc., Wallingford CT, **2009**.

[93] T. Keith, TK Gristmill Software; Overland Park KS, **2011**.

[94] G. Gilli, P. Gilli, *J. Mol. Struct.* **2000**, *552*, 1.

[95] R. M. Badger, *J. Chem. Phys.* **1934**, *2*, 128.

[96] O. Galvez, P. Gomez, L. Pacios, *J. Chem. Phys.* **2001**, *115*, 11166.

[97] E. Espinosa, I. Mata, I. Alkorta, E. Molins, *J. Phys. Chem. A* **2005**, *109*, 2442.

[98] A. Ranganathan, G. Kulkarni, C. Rao, *J. Phys. Chem. A* **2003**, *107*, 6073.

[99] E. D'Oria, J. Novoa, *J. Phys. Chem. A* **2011**, *115*, 13114.

[100] A. Liebschner, C. Jelch, E. Espinosa, C. Lecomte, E. Chabriere, B. Guillot, *J. Phys. Chem. A* **2011**, *115*, 12895.

[101] D. Cremer, J. Gauss, *J. Am. Chem. Soc.* **1986**, *108*, 7467.

[102] Y.-R. Luo, Comprehensive Handbook of Chemical Bond Energies; Taylor & Francis: New York, **2007**.

[103] B. Ault, *Acc. Chem. Res.* **1982**, *109*, 103.

[104] C. C. M. Samson, W. Klopper, *J. Mol. Struct.* (THEOCHEM) **2002**, *586*, 201.

[105] A. Kovacs, Z. Varga, *Coord. Chem. Rev* **2006**, *250*, 710.

[106] S. Smuczynska, P. Skurski, *Chem. Phys. Lett.* **2007**, *443*, 190.

[107] H. Ishibashi, A. Hayashi, M. Shiga, M. Tachikawa, *Chem Phys Chem.* **2008**, *9*, 383.

[108] M. Kaledin, J. Moffitt, C. Clark, F. Rizvi, *J. Chem. Theor. Comp.* **2009**, *5*, 1328.

[109] S. Grabowski, J. Ugalde, *Chem. Phys. Lett.* **2010**, *493*, 37.

[110] J. Stare, *Acta Chim. Slov.* **2011**, *58*, 501.

[111] P. Gilli, V. Bertolasi, V. Ferretti, G. Gilli, *J. Am. Chem. Soc.* **1994**, *116*, 909.

Received: 12 January 2012

Accepted: 13 March 2012

Published online on Wiley Online Library